ACS Medicinal Chemistry Letters

pubs.acs.org/acsmedchemlett
Letter

Discovery of Novel DDR1 Inhibitors through a Hybrid Virtual Screening Pipeline, Biological Evaluation and Molecular Dynamics Simulations

Xinglong Chi,[#] Roufen Chen,[#] Xinle Yang, Xinjun He, Zhichao Pan, Chenpeng Yao, Huilin Peng, Haiyan Yang,* Wenhai Huang,* and Zhilu Chen*

Cite This: ACS Med. Chem. Lett. 2025, 16, 602−610

ABSTRACT: Acute myeloid leukemia (AML) is a heterogeneous hematopoietic malignancy with limited therapeutic options for many patients. Discoidin domain receptor 1 (DDR1), a transmembrane tyrosine kinase receptor, has been implicated in AML progression and represents a promising therapeutic target. In this study, we employed a hybrid virtual screening workflow that integrates deep learning-based binding affinity predictions with molecular docking techniques to identify potential DDR1 inhibitors. A multistage screening process involving PSICHIC, KarmaDock, Vina-GPU, and similarity-based scoring was conducted, leading to the selection of seven candidate compounds. The biological evaluation identified Compound 4 as a novel DDR1 inhibitor, demonstrating significant DDR1 inhibitory activity with an IC_{50} of 46.16 nM and a 99.86% inhibition rate against Z-138 cells at 10 μM. Molecular dynamics simulations and binding free energy calculations further validated the stability and strong binding interactions of Compound 4 with DDR1. This study highlights the utility of combining deep learning models with traditional molecular docking techniques to accelerate the discovery of potent and selective DDR1 inhibitors. The identified compounds hold promise for further development as targeted therapies for AML.

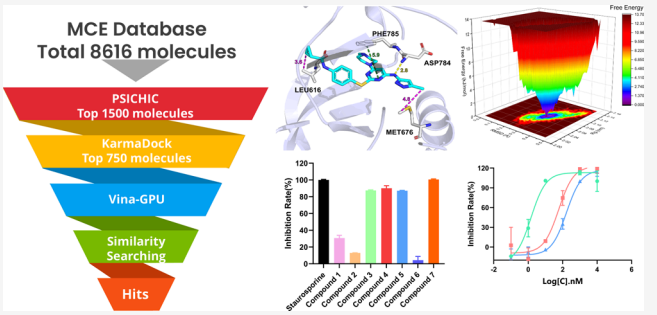

KEYWORDS: *DDR1, AML, Virtual Screening, Deep Learning, Molecular Dynamics*

Acute myeloid leukemia (AML) is a malignant tumor of the hematopoietic system originating from myeloid precursor cells, with a high degree of heterogeneity.[1] Intensive chemotherapy is recommended as the first choice for patients with newly diagnosed AML. Low-dose cytarabine (LDAC) and hypomethylating agents (HMAs) are recommended for patients who cannot tolerate intensive chemotherapy.[2] The (7 + 3) induction intensive chemotherapy containing cytarabine and anthracyclines is the traditional first-line regimen for AML. Allogeneic stem cell transplantation (Allo-SCT) is a breakthrough treatment for improving survival in AML patients. Nevertheless, less than 50% of patients are suitable for first-line induction chemotherapy, and not all patients are eligible for transplantation, both of which make drug choices limited. With further studies of the AML genome and molecular mutations, targeted therapies and combinations of different classes of therapeutic agents could further improve patient survival rates.[3] Currently, there is still a substantial unmet need for the treatment of AML. Inhibitor development based on disease-specific targets in AML patients facilitates genuinely personalized therapy.

Discoidin domain receptors (DDR) are a special type of transmembrane tyrosine kinase receptors (RTKS),[4] which are aberrantly expressed in many human cancers. DDR includes DDR1 and DDR2, which play a series of biological roles by binding to collagen. They can regulate cell proliferation, adhesion, migration, and matrix remodeling. Dysregulation of receptors may promote cancer progression.[5] In AML, somatic mutations of the DDR1 gene have been reported.[6] In addition, several studies have found that the expression level of DDR1 is elevated in AML, indicating that DDR1 may be related to the disease progression of AML.[7,8]

When collagen binds to the DS domain of the receptor, DDR1 is activated and phosphorylated. Usually, RTK participates in the development of AML by regulating the PI3K/AKT pathway and affecting c-MYC transcription.[9] DDR1 exerts its effects by binding to collagen, further regulating cell dynamic behavior, matrix remodeling, and

Received: December 30, 2024
Revised: January 18, 2025
Accepted: February 20, 2025
Published: March 17, 2025

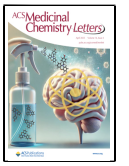

https://doi.org/10.1021/acsmedchemlett.4c00634
ACS Med. Chem. Lett. 2025, 16, 602−610

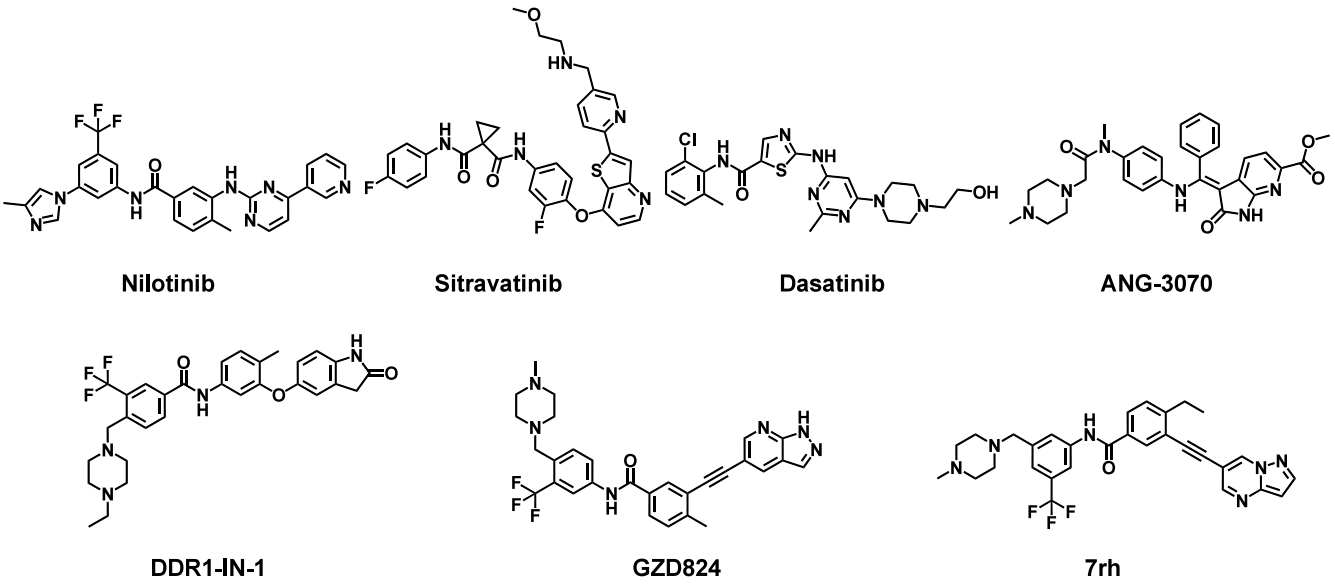

Figure 1. Structure of reported DDR1 inhibitors.

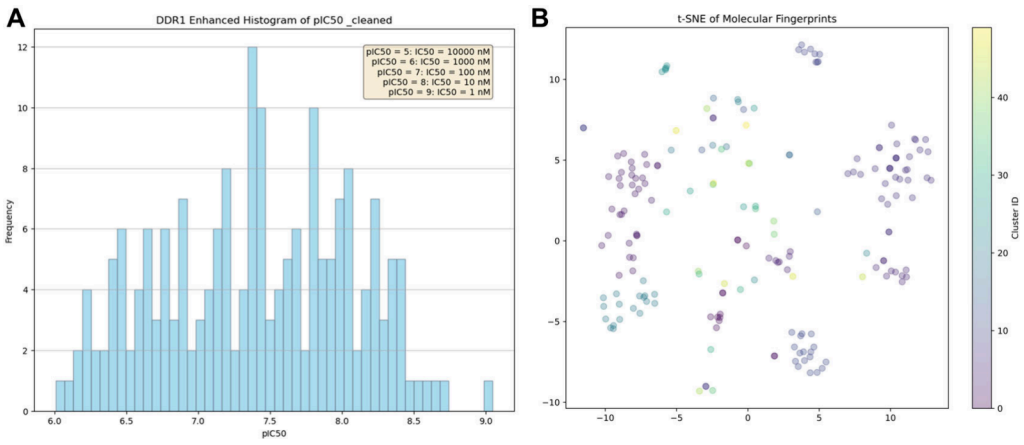

Figure 2. Distribution of the DDR1 active data set. (A) The pIC_{50} distribution of DDR1 active compounds. (B) The t-SNE plot of DDR1 active data set.

mediating cell signaling pathways.[10] Some studies support that the upregulation of DDR1 facilitates AML tumor cell migration and invasion into extramedullary sites, thereby promoting AML progression. In addition, the expression of DDR1 helps to build a barrier around the tumor, limiting the effect of T cells in killing tumor cells.[11] If a suitable DDR1 inhibitor can be found, it may become a new strategy for treating AML.

Drugs targeting DDR1 have been extensively studied, primarily in the field of oncology,[12] with a focus on DDR1 antagonists. Several DDR1 inhibitors, including nilotinib, dasatinib, and GZD824, have been approved for clinical use.[13] Additionally, sitravatinib and ANG-3070 are currently in Phase III and Phase II clinical trials, respectively.[14] Other inhibitors, such as DDR1-1N-1 and 7rh, remain in the developmental stage and have not yet reached clinical application (Figure 1). Despite the promising efficacy of these candidate drugs, challenges such as off-target effects and inconsistent therapeutic outcomes limit their clinical utility. While DDR1 inhibitors are an active area of research and development, there is a noticeable absence of highly effective DDR1 inhibitors in widespread clinical use.[15] Furthermore, the evaluation of multitarget inhibitors remains complex due to their associated adverse effects. Therefore, it is crucial to accelerate and broaden drug screening efforts to identify potent and stable DDR1 inhibitors that can overcome these limitations and achieve consistent clinical efficacy and safety.

In response to the limitations of traditional DDR1 inhibitors, we focused on discovering new DDR1 inhibitors. We developed a novel method for inhibitor discovery that combines deep learning with molecular docking techniques. This innovative approach allowed us to identify a new class of DDR1 inhibitors with scaffolds distinct from those of conventional DDR1 inhibitors. Our method involved constructing a comprehensive DDR1 data set, applying deep learning models to predict binding affinity from sequence data directly, and using an ensemble molecular docking strategy for virtual screening. Compound 4 exhibited DDR1 inhibitory activity among the compounds identified, with an IC_{50} of 46.16 nM.

Furthermore, this compound significantly reduced cell viability in hematologic tumor cell lines, as shown by cell viability assays. Molecular dynamics simulations were also conducted to analyze the binding stability and interactions of

https://doi.org/10.1021/acsmedchemlett.4c00634
ACS Med. Chem. Lett. 2025, 16, 602−610

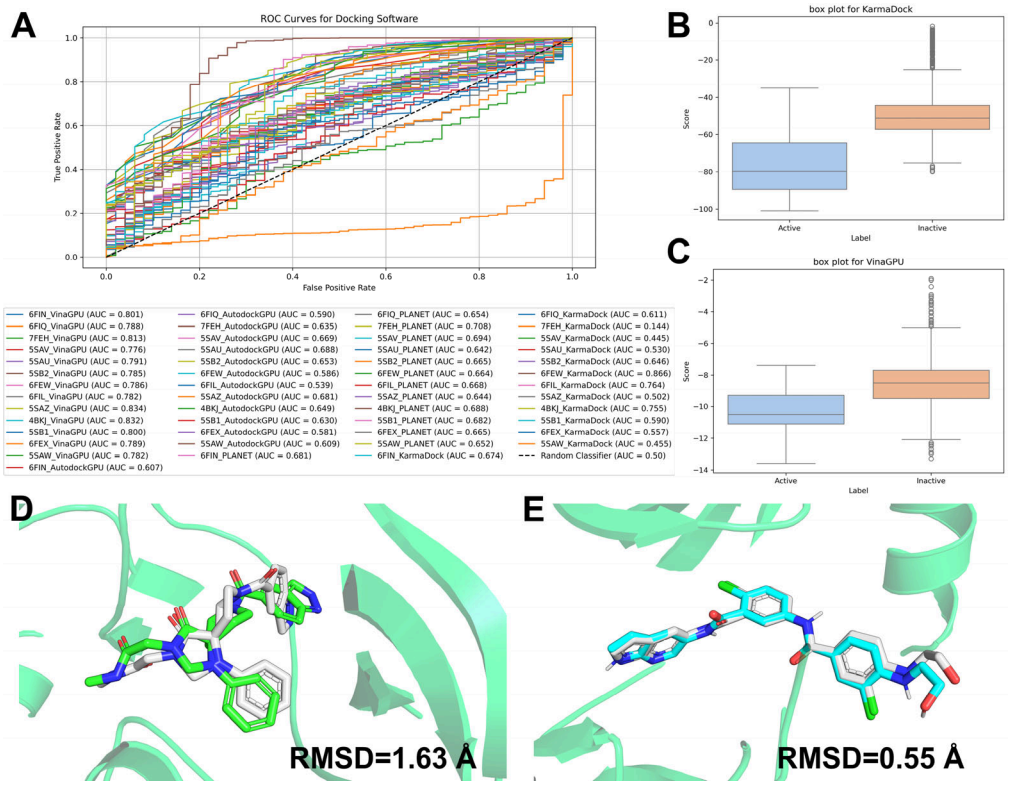

Figure 3. Evaluation results of docking programs and DDR1 proteins. (A) The ROC curve for the molecular docking of multiple DDR1 proteins with the selected docking programs using DDR1 validation data set. (B) The box plot of KarmaDock with 6FEW protein. (C) The box plot of Vina-GPU with 5SAZ protein. (D) The redocking result of DDR1 protein (PDB ID: 6FEW) using KarmaDock (White: original structure; Green: redocking conformation). (E) The redocking result of DDR1 protein (PDB ID: 5SAZ) using Vina-GPU (White: original structure; Blue: redocking conformation).

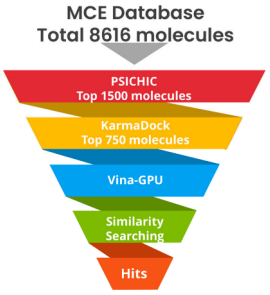

Figure 4. Hybrid Virtual Screening workflow of DDR1 inhibitor discovery.

Compound 4 with DDR1. These simulations confirmed the high binding affinity of Compound 4 and elucidated its mechanism of action, suggesting its potential for further development as a therapeutic agent.

We obtained DDR1 active molecules with reported pIC_{50} values of 6 or higher from the ChEMBL database[16,17] to serve as the active molecule component of the validation data set. These molecules were carefully selected based on their documented bioactivity against DDR1 to ensure high-quality data for downstream validation. To account for structural diversity within the data set, we clustered the active molecules into 50 distinct groups using structural similarity metrics. For each cluster, a representative compound was chosen, serving as a reference for the generation of decoy molecules. Decoys were generated using the advanced deep learning tool DeepCoy,[18] which is specifically designed to produce structurally similar but biologically inactive compounds. This approach ensures the validation data set is well-balanced, comprising both active and decoy molecules for robust performance evaluation of predictive models. As a result, the final validation data set included 50 active molecules and 2,450 decoy molecules, providing a comprehensive set of compounds to test the accuracy and specificity of virtual screening tools. Furthermore, the distribution of pIC_{50} values across the active molecules and the detailed clustering results were visualized, as shown in Figure 2.

Using the integrated tool EvaluationMaster[19] from GitHub, we systematically evaluated the performance of four docking software programs—AutoDock-GPU,[20,21] Vina-GPU,[22] PLANET,[23] and KarmaDock[24]—across 13 DDR1 protein structures with resolutions of 2.5 Å or better from RCSB database.[25] The results, presented in Figure 3A, identified the combination of KarmaDock and the 6FEW protein structure as the top-performing pair, achieving a ROC-AUC of 0.866. This high ROC-AUC value[26,27] indicates excellent discrimination between DDR1 active and inactive molecules. To further analyze the statistical significance of these results, we conducted *t* tests. The KarmaDock-6FEW combination produced a t-value of −15.19 and a p-value of 6.38×10^{-50}. The low p-values indicate a significant distinction between the active and inactive molecule classifications for both combinations, with KarmaDock-6FEW exhibiting the best statistical performance. Additionally, the box plots shown in Figure 3B visually highlight the effectiveness of these combinations. KarmaDock, in particular, demonstrated an effective separation of DDR1 active molecules from inactive ones.

https://doi.org/10.1021/acsmedchemlett.4c00634
ACS Med. Chem. Lett. 2025, 16, 602−610

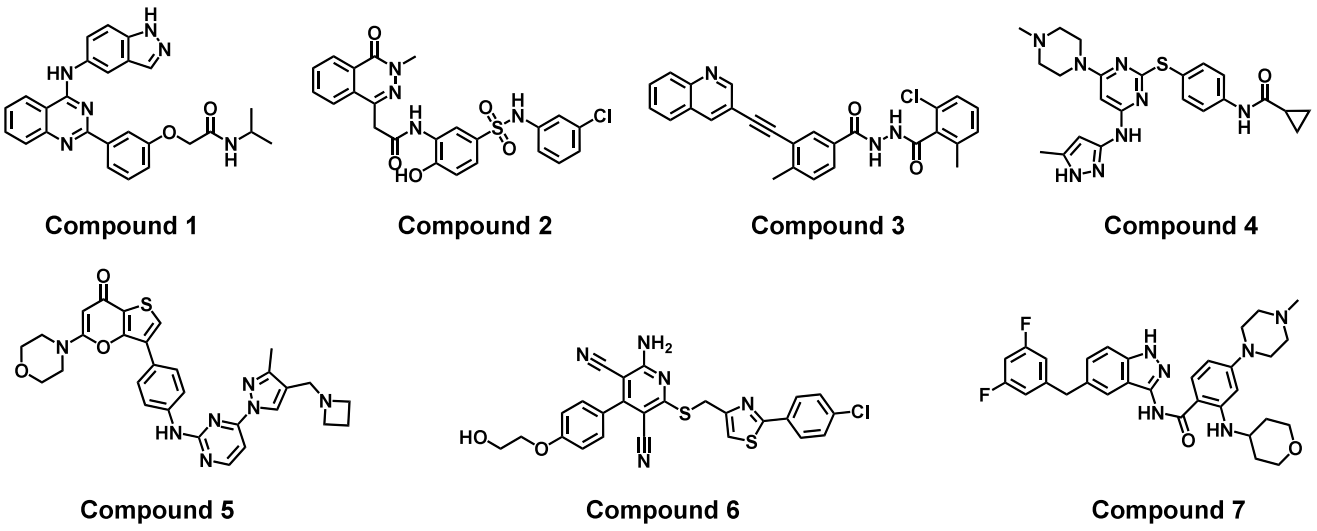

Figure 5. Structure of screened 7 molecules.

Table 1. Screening Score Result of Screened 7 Compounds

Entry	PSICHIC Affinity	KarmaDock Score	Vina-GPU Score	Similarity Score	@25 μM Inhibition Rate (%)
Compound 1	8.120	79.977	−10.5	0.367	30.69 ± 3.28
Compound 2	7.894	96.555	−10.8	0.323	12.92 ± 0.10
Compound 3	8.038	99.111	−13.5	0.479	87.46 ± 0.71
Compound 4	7.904	64.292	−7.9	0.350	90.10 ± 3.04
Compound 5	7.924	73.703	−8.9	0.354	87.12 ± 0.46
Compound 6	8.059	72.766	−9.0	0.272	4.35 ± 4.40
Compound 7	8.014	83.394	−11.1	0.329	100.57 ± 0.66
Staurosporine[a]	–	–	–	–	100.06 ± 0.56

[a]This entry in the table represents the positive control compound used in the enzyme inhibition assay at 25 μM.

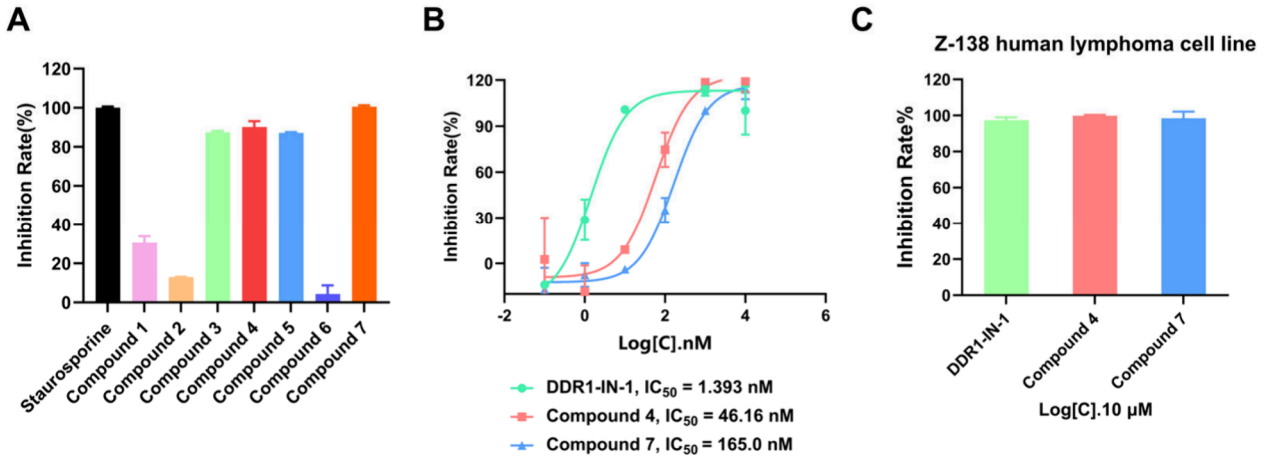

Figure 6. Biological evaluation results of Compound 4 and Compound 7. (A) The inhibition rate histogram of screened 7 molecules (positive reference: Staurosporine). (B) The dose−response curves for Compound 4 and Compound 7 (positive reference: DDR1-IN-1). (C) The cell inhibition results for the Z-138 cell line treated with Compound 4 and Compound 7 (positive reference: DDR1-IN-1).

Although KarmaDock demonstrated excellent discrimination ability on the DDR1 target, it has a known limitation in generating accurate ligand conformations, often resulting in structural errors. In contrast, Vina-GPU is capable of generating more accurate ligand conformations. In the evaluation using the 5SAZ complex, Vina-GPU achieved a ROC-AUC of 0.834, with a t-value of −9.20 and a p-value of 7.48×10^{-20}, indicating strong statistical significance. The corresponding box plot further confirmed its robust discrimination ability. Therefore, to ensure the accuracy of the ligand conformations used in subsequent molecular dynamics (MD) simulations, we selected Vina-GPU as the final screening method following KarmaDock.

To further evaluate the effectiveness of the docking software, redocking experiments were conducted using KarmaDock and Vina-GPU with their respective proteins and crystallographic ligands. As shown in Figure 3D and 3E, the redocking results demonstrated that the conformations predicted by Vina-GPU

https://doi.org/10.1021/acsmedchemlett.4c00634
ACS Med. Chem. Lett. 2025, 16, 602−610

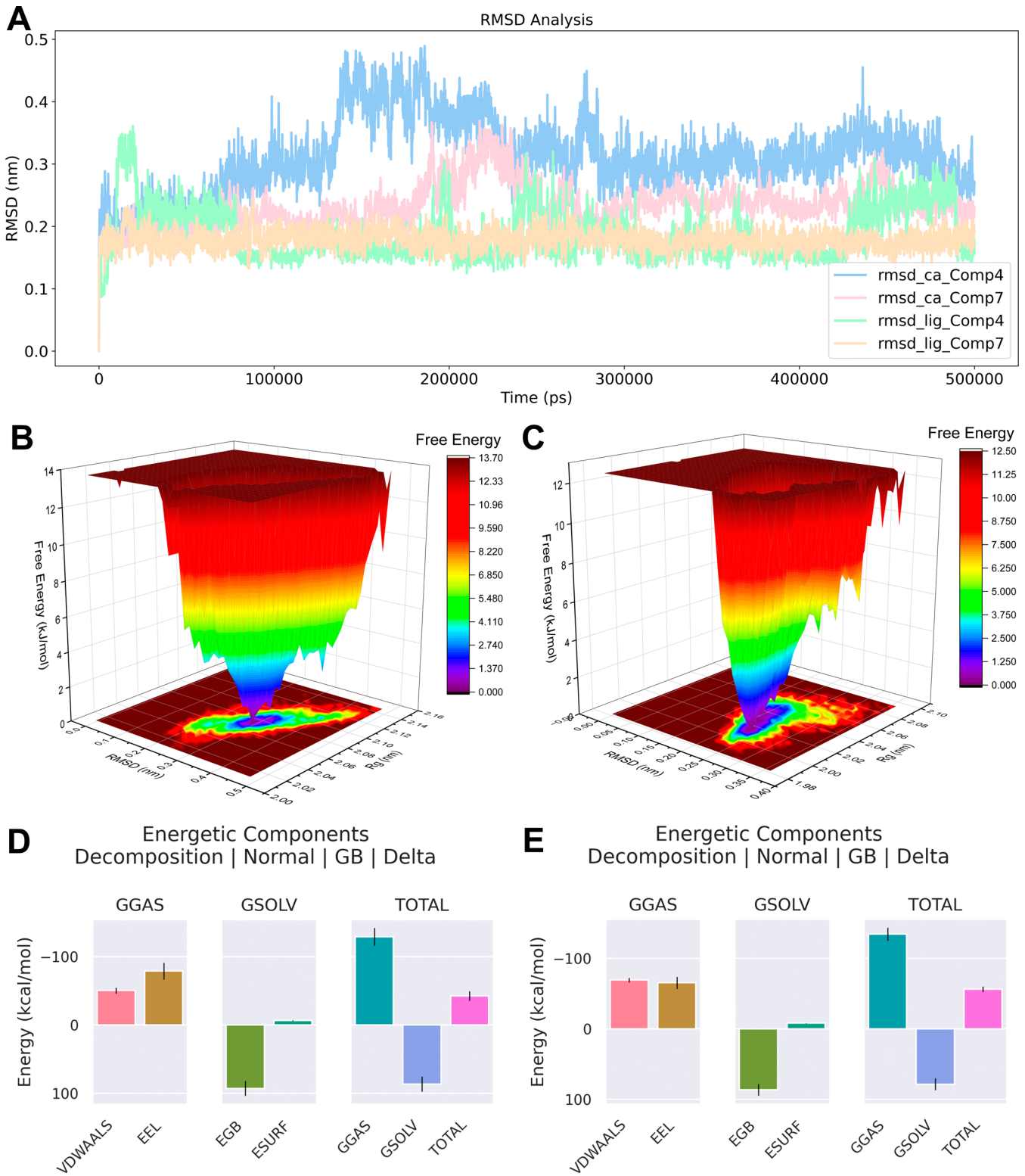

Figure 7. RMSD trajectory and total energy analysis of MD results of Compound 4 and Compound 7 with DDR1 protein. (A) The RMSD trajectory of DDR1-Compound 4 complex and DDR1-Compound 7 complex for 500 ns. (B) The Gibbs freedom energy landscape of DDR1-Compound 4 complex. (C) The Gibbs freedom energy landscape of DDR1-Compound 7 complex. (D) The total binding free energy of complex of Compound 4 with DDR1 protein. (E) The total binding free energy of complex of Compound 7 with DDR1 protein.

were almost identical to the initial crystallographic poses, while those predicted by KarmaDock closely aligned with the backbone of the original structures. The Root Mean Square Deviation (RMSD) between the original and redocked conformations was calculated using OpenBabel,[28] yielding an RMSD of 0.55 Å for Vina-GPU and 1.63 Å for KarmaDock. Since an RMSD below 2 Å is generally considered to indicate reliable redocking performance, these results suggest that both KarmaDock and Vina-GPU exhibit high accuracy and reliability. Consequently, KarmaDock was selected for the

https://doi.org/10.1021/acsmedchemlett.4c00634
ACS Med. Chem. Lett. 2025, 16, 602−610

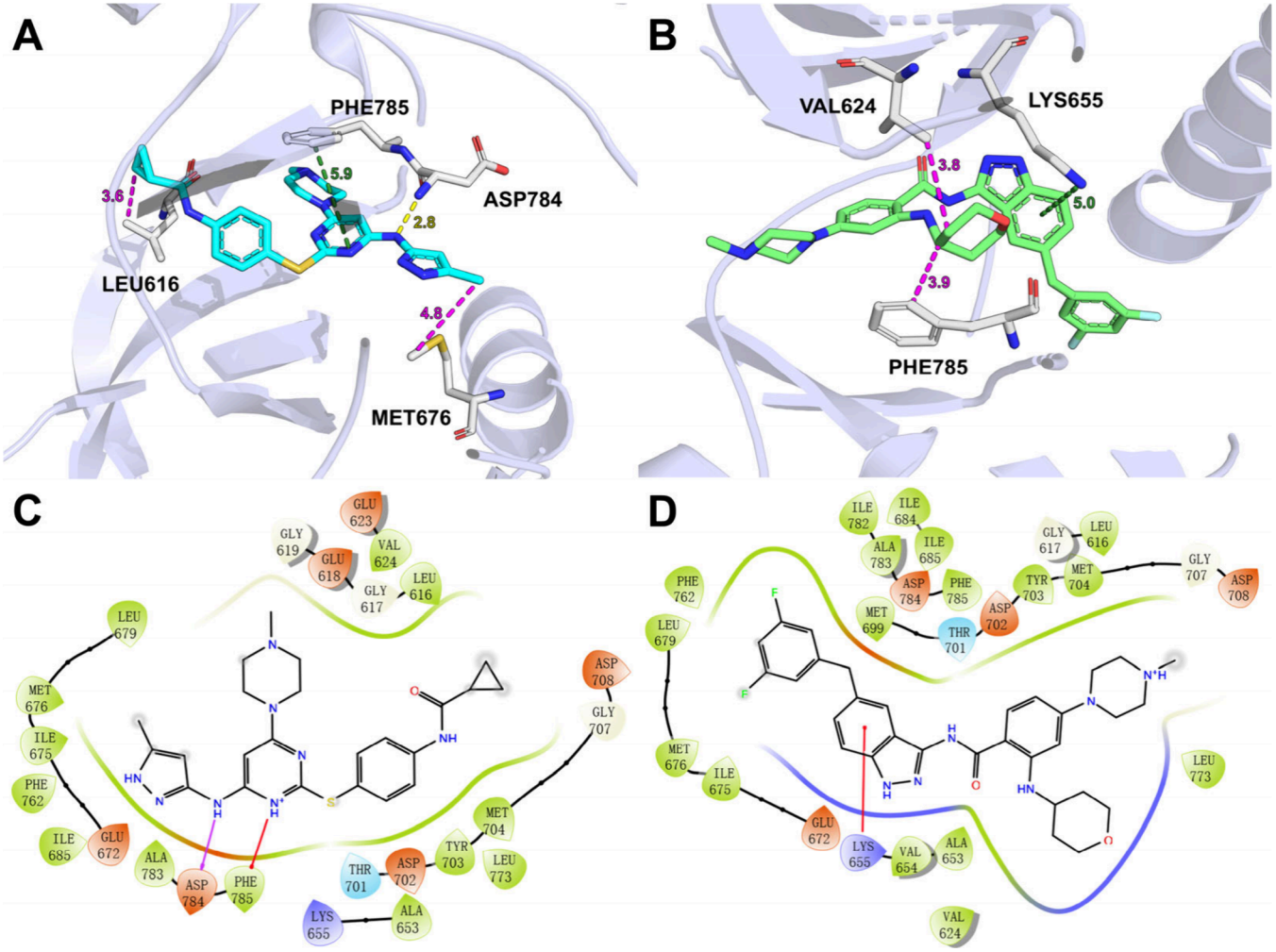

Figure 8. Detail binding mode analysis of Compound 4 and Compound 7 after 500 ns MD. (A) The 3D binding mode of Compound 4 and DDR1 protein. (B) The 3D binding mode of Compound 7 and DDR1 protein. (C) The 2D binding mode of Compound 4 with DDR1 protein (Purple: hydrogen bond; Red: p-π interaction). (D) The 2D binding mode of Compound 7 with DDR1 protein (Red: p-π interaction).

second round of virtual screening, while Vina-GPU was chosen for the third round.

We developed a hybrid virtual screening workflow to identify potential DDR1 inhibitors using a library of MCE-like drug compounds.[29] The library was prepared with RDKit,[30] and previously reported DDR1 active molecules were excluded to ensure novelty. After this curation process, the virtual screening workflow included a total of 8,616 compounds.

The hybrid screening workflow is illustrated in Figure 4. We first employed PSICHIC[31] to predict the binding affinities of compounds to the DDR1 protein directly from protein sequences and molecular SMILES representations.[32,33] This initial computational screening identified 1,500 compounds with affinity scores exceeding 7.649, which were subsequently selected for the second round of docking-based screening using KarmaDock. In this stage, compounds with KarmaDock scores above 63.79 were further refined to a subset of 750 molecules for the third round of screening using Vina-GPU docking, followed by a fourth round of similarity-based scoring.[34]

Following these computational steps, the final selection of seven compounds was made based on visual inspection by medicinal chemists, considering the alignment of docking poses and chemical features with the target binding site. These seven compounds were chosen for experimental validation of biological activity. The molecular structures are shown in Figure 5, while corresponding scores from each screening round are summarized in Table 1, providing a comprehensive overview of the compound selection process and their performance throughout the workflow.

The biological evaluation of the selected compounds was performed using the ADP-Glo assay to measure their inhibition rates against DDR1 at a concentration of 25 μM. As shown in Figure 6A, Compound 7 exhibited the highest inhibition rate of 100.57%, followed by Compound 4, which achieved an inhibition rate of 90.10%. The positive control, Staurosporine, displayed a comparable inhibition rate of 100.06%. IC_{50} values were determined to further assess these compounds' potency, and the corresponding dose−response curves for Compound 4, Compound 7, and the positive control DDR1-IN-1 were presented in Figure 6B. Compound 7 demonstrated notable inhibitory activity against DDR1 with an IC_{50} value of 165.0 nM, while Compound 4 showed an IC_{50} value of 46.16 nM. In comparison, the positive control DDR1-IN-1 exhibited superior potency, with an IC_{50} value of 1.393 nM.

Additionally, the cell viability of hematologic tumor cell lines treated with Compound 4, Compound 7, and DDR1-IN-1 was

https://doi.org/10.1021/acsmedchemlett.4c00634
ACS Med. Chem. Lett. 2025, 16, 602−610

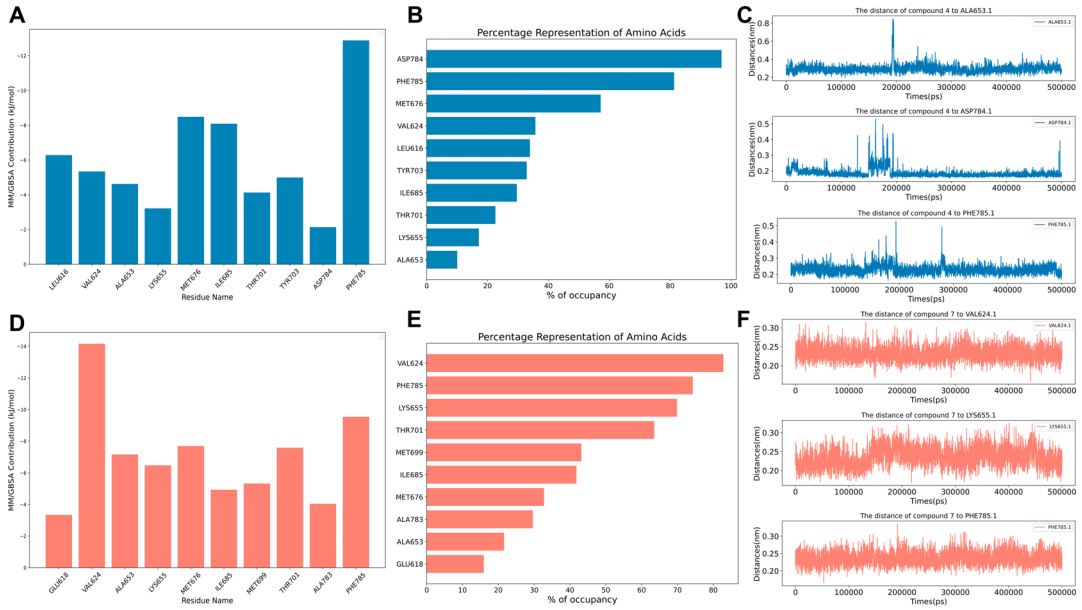

Figure 9. Contribution to Gibbs energy analysis of different residues of DDR1 protein. (A) The contribution analysis of amino acid residues for DDR1 protein (Compound 4). (B) The occupancy percentage of binding between Compound 4 and DDR1 protein. (C) The binding distances between Compound 4 and different DDR1 proteins. (D) The contribution analysis of amino acid residues for DDR1 protein (Compound 7). (E) The occupancy percentage of binding between Compound 7 and DDR1 protein. (F) The binding distances between Compound 7 and different DDR1 proteins.

evaluated, and the results are depicted in Figure 6C. The cell viability assay revealed that both Compound 4 and Compound 7 significantly reduced cell viability in the tested Z-138 human lymphoma cell line, demonstrating efficacy comparable to DDR1-IN-1. Collectively, these results indicate that the selected compounds effectively inhibit DDR1 at the molecular level and exhibit significant biological activity in cell-based assays, suggesting their potential for further development as DDR1 inhibitors for AML therapeutic agents.

Building on the inhibitory activity assessments, molecular dynamics (MD) simulations of the DDR1-Compound 4 and DDR1-Compound 7 complexes were conducted to investigate their binding interactions, providing insights for further structural optimization. The simulations were performed using GROMACS 2021.06.[35,36] As shown in Figure 7A, the binding of both compounds to DDR1 stabilized after 300 ns of simulation, indicating that the system had reached equilibrium and was suitable for subsequent analyses.

Further analysis using the free energy surface (FES) validated the stability of these binding modes (Figures 7B and 7C). The FES plot illustrates the relationship between root-mean-square deviation (RMSD), radius of gyration (Rg), and free energy. For Compound 4, binding to DDR1 stabilized the system in a low-free-energy region (depicted in deep blue), indicating a strong binding affinity with an RMSD of 0.30 nm and an Rg of 2.07 nm. Similarly, Compound 7 binding stabilized a low-free-energy region, with an RMSD of 0.23 nm and an Rg of 2.02 nm. These free energy minima highlight the robust and stable interactions between DDR1 and both two compounds. These findings were further corroborated by binding free energy calculations using the MM/GBSA method.[37−39] The binding free energy of Compound 4 was determined to be -42.61 kcal/mol (Figure 7D), while that of Compound 7 was -56.34 kcal/mol (Figure 7E). These values confirm the strength of the protein−ligand interactions.

The final frame from the MD simulation was extracted to analyze the specific interactions between DDR1 and Compounds 4 and 7. As shown in Figure 8A, Compound 4 forms a hydrogen bond with ASP784 within the DDR1 binding pocket, establishes a p-π interaction with PHE785, and engages in hydrophobic interactions with residues such as LEU616 and MET676. At the same time, Compound 7 primarily interacts with LYS655 through a p-π interaction, forming hydrophobic interactions with VAL624, PHE785, and other residues. The 2D interaction diagrams (Figures 8C and 8D) further confirm these interactions, which align with previously reported critical amino acids in the DDR1 binding pocket, including LYS655, ASP784, and PHE785.[40,41]

Further, we utilized the gmx_MMGBSA tool to calculate the contribution of individual amino acid residues to the binding free energy. As shown in Figure 9A, MET676 and PHE785 were identified as key contributors to the binding energy of the DDR1-Compound 4 complex. Additional analysis of the occupancy rates of critical amino acids during the simulation (Figure 9B) and the distance fluctuations between these residues and the ligand (Figure 9C) revealed that ASP784 and PHE785 exhibited high occupancy values of 96.88% and 81.3%, respectively. Moreover, their distances from the ligand remained consistently below 3 Å, indicating strong and stable interactions throughout the simulation.

At the same time, for the DDR1-Compound 7 complex, VAL624, LYS655, and PHE785 were found to significantly contribute to the binding energy (Figure 9D). Analysis of the simulation data (Figure 9E) showed that these residues maintained high occupancy values during the simulation, with VAL624 at 82.80%, PHE785 at 74.29%, and LYS655 at 69.87%. The distance fluctuations between these residues and Compound 7 also remained stable, consistently below 3 Å (Figure 9F), further supporting the stability of these interactions.

https://doi.org/10.1021/acsmedchemlett.4c00634
ACS Med. Chem. Lett. 2025, 16, 602−610

These findings align with previous analyses, reinforcing the critical roles of ASP784, PHE785, MET676, VAL624, and LYS655 in mediating the interactions between DDR1 and the selected compounds. The consistent proximity and substantial contributions of these residues to the binding energy underscore the stability of the DDR1-Compound 4 and DDR1-Compound 7 complexes.

In summary, we employed a hybrid virtual screening approach that integrates deep learning-based binding affinity predictions with molecular docking techniques to identify potential high-affinity DDR1 inhibitors for treating AML. Our innovative strategy successfully identified a novel DDR1 inhibitor, Compound 4, which demonstrated significant DDR1 inhibitory activity (IC_{50} = 46.16 nM) and exhibited notable cytotoxic effects on the Z-138 cell line at a concentration of 10 μM (inhibition rate = 99.86%). To ensure the robustness and accuracy of the screening process, we rigorously evaluated molecular docking software and protein structures. Additionally, biological validation and molecular dynamics simulations confirmed the selected compound's high binding affinity, stability, and mechanism of action. These findings highlight the potential of combining deep learning models with traditional molecular docking methods to advance the development of DDR1 inhibitors and offer a promising strategy for targeted therapeutic discovery.

■ ASSOCIATED CONTENT

Supporting Information

The Supporting Information is available free of charge at https://pubs.acs.org/doi/10.1021/acsmedchemlett.4c00634.

Tables and figures, materials and methods, docking score of each phase, purity and spectrogram data of tested compounds (PDF)

■ AUTHOR INFORMATION

Corresponding Authors

Haiyan Yang − *Department of Lymphoma, Zhejiang Cancer Hospital, Hangzhou 310022, China*; Email: yanghy@zjcc.org.cn

Wenhai Huang − *Affiliated Yongkang First People's Hospital and School of Pharmaceutical Sciences, Hangzhou Medical College, Hangzhou 310053, P.R. China*; orcid.org/0000-0003-1457-7380; Email: hwh@hmc.edu.cn

Zhilu Chen − *Department of Hematology, Tongde Hospital of Zhejiang Province, Hangzhou 310012 Zhejiang, P.R. China*; Email: zhiluChen123@outlook.com

Authors

Xinglong Chi − *Department of Hematology, Tongde Hospital of Zhejiang Province, Hangzhou 310012 Zhejiang, P.R. China; Affiliated Yongkang First People's Hospital and School of Pharmaceutical Sciences, Hangzhou Medical College, Hangzhou 310053, P.R. China*

Roufen Chen − *College of Pharmaceutical Sciences, Zhejiang University, Hangzhou 310058, China*

Xinle Yang − *College of Pharmaceutical Sciences, Zhejiang University of Technology, Hangzhou 310014, China*

Xinjun He − *College of Pharmaceutical Sciences, Zhejiang University, Hangzhou 310058, China*

Zhichao Pan − *College of Pharmaceutical Sciences, Zhejiang University, Hangzhou 310058, China*

Chenpeng Yao − *College of Pharmaceutical Sciences, Zhejiang University, Hangzhou 310058, China*

Huilin Peng − *Department of Lymphoma, Zhejiang Cancer Hospital, Hangzhou 310022, China*

Complete contact information is available at: https://pubs.acs.org/10.1021/acsmedchemlett.4c00634

Author Contributions

#X.C. and R.C. contributed equally to this work.

Notes

The authors declare no competing financial interest.

■ ACKNOWLEDGMENTS

The authors sincerely thank ICE Bioscience Inc. for their support and for conducting the biological activity testing essential to this research. The dynamic experiments in this study were supported by the Information Technology Center and the State Key Laboratory of CAD&CG, Zhejiang University.

■ ABBREVIATIONS

DDR1, Discoidin domain receptor 1; AML, Acute myeloid leukemia; LDAC, Low-dose cytarabine; HMAs, hypomethylating agents; Allo-SCT, Allogeneic stem cell transplantation; RMSD, Root Mean Square Deviation; MD, Molecular dynamics; MMGBSA, Molecular mechanics with generalized Born and surface area.

■ REFERENCES

(1) Mohamed Jiffry, M. Z.; et al. A review of treatment options employed in relapsed/refractory AML. *Hematology* **2023**, *28*, 2196482.

(2) Heuser, M.; et al. Therapies for acute myeloid leukemia in patients ineligible for standard induction chemotherapy: a systematic review. *Future Oncol* **2023**, *19*, 789−810.

(3) Liu, H. Emerging agents and regimens for AML. *Journal of hematology & oncology* **2021**, *14*, 49.

(4) Gao, Y.; Zhou, J.; Li, J. Discoidin domain receptors orchestrate cancer progression: A focus on cancer therapies. *Cancer Sci.* **2021**, *112*, 962−969.

(5) Matada, G. S. P.; Das, A.; Dhiwar, P. S.; Ghara, A. DDR1 and DDR2: a review on signaling pathway and small molecule inhibitors as an anticancer agent. *Medicinal Chemistry Research* **2021**, *30*, 535−551.

(6) Tomasson, M. H.; et al. Somatic mutations and germline sequence variants in the expressed tyrosine kinase genes of patients with de novo acute myeloid leukemia. *Blood* **2008**, *111*, 4797−4808.

(7) Favreau, A. J.; Cross, E. L.; Sathyanarayana, P. miR-199b-5p directly targets PODXL and DDR1 and decreased levels of miR-199b-5p correlate with elevated expressions of PODXL and DDR1 in acute myeloid leukemia. *Am. J. Hematol* **2012**, *87*, 442−446.

(8) Favreau, A. J.; Vary, C. P.; Brooks, P. C.; Sathyanarayana, P. Cryptic collagen IV promotes cell migration and adhesion in myeloid leukemia. *Cancer Med.* **2014**, *3*, 265−272.

(9) Carter, J. L.; et al. Targeting multiple signaling pathways: the new approach to acute myeloid leukemia therapy. *Signal Transduct Target Ther* **2020**, *5*, 288.

(10) Tian, Y.; Bai, F.; Zhang, D. New target DDR1: A "double-edged sword" in solid tumors. *Biochimica et Biophysica Acta (BBA) - Reviews on Cancer* **2023**, *1878*, No. 188829.

(11) Sun, X.; et al. Tumour DDR1 promotes collagen fibre alignment to instigate immune exclusion. *Nature* **2021**, *599*, 673−678.

(12) Martorana, F.; Da Silva, L. A.; Sessa, C.; Colombo, I. Everything Comes with a Price: The Toxicity Profile of DNA-Damage Response Targeting Agents. *Cancers (Basel)* **2022**, *14*, 953.

(13) Nokin, M. J. Inhibition of DDR1 enhances in vivo chemosensitivity in KRAS-mutant lung adenocarcinoma. *JCI Insight* **2020**, *5*, e137869 DOI: 10.1172/jci.insight.137869.
(14) Dong, R.; et al. Discovery of 4-amino-1H-pyrazolo[3,4-d]pyrimidin derivatives as novel discoidin domain receptor 1 (DDR1) inhibitors. *Bioorg. Med. Chem.* **2021**, *29*, No. 115876.
(15) Wu, D.; et al. DDR1-targeted therapies: current limitations and future potential. *Drug Discov Today* **2024**, *29*, No. 103975.
(16) Padalino, G. Using ChEMBL to Complement Schistosome Drug Discovery. *Pharmaceutics* **2023**, *15*, 1359.
(17) Zdrazil, B.; et al. The ChEMBL Database in 2023: a drug discovery platform spanning multiple bioactivity data types and time periods. *Nucleic Acids Res.* **2024**, *52*, D1180−D1192.
(18) Imrie, F.; Bradley, A. R.; Deane, C. M. Generating property-matched decoy molecules using deep learning. *Bioinformatics* **2021**, *37*, 2134−2141.
(19) Shen, Z.; et al. EvaluationMaster: A GUI Tool for Structure-Based Virtual Screening Evaluation Analysis and Decision-Making Support. *J. Chem. Inf Model* **2025**, *65*, 7.
(20) El-Hachem, N.; Haibe-Kains, B.; Khalil, A.; Kobeissy, F. H.; Nemer, G. AutoDock and AutoDockTools for Protein-Ligand Docking: Beta-Site Amyloid Precursor Protein Cleaving Enzyme 1(BACE1) as a Case Study. *Methods Mol. Biol.* **2017**, *1598*, 391−403.
(21) Santos-Martins, D.; et al. Accelerating AutoDock4 with GPUs and Gradient-Based Local Search. *J. Chem. Theory Comput* **2021**, *17*, 1060−1073.
(22) Ding, J.; et al. Vina-GPU 2.0: Further Accelerating AutoDock Vina and Its Derivatives with Graphics Processing Units. *J. Chem. Inf Model* **2023**, *63*, 1982−1998.
(23) Zhang, X. PLANET: A Multi-objective Graph Neural Network Model for Protein-Ligand Binding Affinity Prediction. *J. Chem. Inf Model* **2024**, 2205.
(24) Zhang, X.; et al. Efficient and accurate large library ligand docking with KarmaDock. *Nat. Comput. Sci.* **2023**, *3*, 789−804.
(25) Goodsell, D. S.; et al. RCSB Protein Data Bank: Enabling biomedical research and drug discovery. *Protein Sci.* **2020**, *29*, 52−65.
(26) Truchon, J. F.; Bayly, C. I. Evaluating virtual screening methods: good and bad metrics for the "early recognition" problem. *J. Chem. Inf Model* **2007**, *47*, 488−508.
(27) Wang, Z.; et al. Comprehensive evaluation of ten docking programs on a diverse set of protein-ligand complexes: the prediction accuracy of sampling power and scoring power. *Phys. Chem. Chem. Phys.* **2016**, *18*, 12964−12975.
(28) O'Boyle, N. M.; et al. Open Babel: An open chemical toolbox. *J. Cheminform* **2011**, *3*, 33.
(29) Thai, Q. M.; et al. MedChemExpress compounds prevent neuraminidase N1 via physics- and knowledge-based methods. *RSC Adv.* **2024**, *14*, 18950−18956.
(30) Lovric, M.; Molero, J. M.; Kern, R. PySpark and RDKit: Moving towards Big Data in Cheminformatics. *Mol. Inform* **2019**, *38*, No. e1800082.
(31) Koh, H. Y.; Nguyen, A. T. N.; Pan, S.; May, L. T.; Webb, G. I. Physicochemical graph neural network for learning protein−ligand interaction fingerprints from sequence data. *Nature Machine Intelligence* **2024**, *6*, 673−687.
(32) McGibbon, M. From intuition to AI: evolution of small molecule representations in drug discovery. *Brief Bioinform* **2023**, *25*, bbad422 DOI: 10.1093/bib/bbad422.
(33) Fang, S., Liu, Y., Liu, S. In *2023 IEEE International Conference on Bioinformatics and Biomedicine (BIBM).*; 3004−3011.
(34) Vazquez, J.; Lopez, M.; Gibert, E.; Herrero, E.; Luque, F. J. Merging Ligand-Based and Structure-Based Methods in Drug Discovery: An Overview of Combined Virtual Screening Approaches. *Molecules* **2020**, *25*, 4723.
(35) Kohnke, B.; Kutzner, C.; Grubmuller, H. A GPU-Accelerated Fast Multipole Method for GROMACS: Performance and Accuracy. *J. Chem. Theory Comput* **2020**, *16*, 6938−6949.
(36) Loschwitz, J.; et al. Dataset of AMBER force field parameters of drugs, natural products and steroids for simulations using GROMACS. *Data Brief* **2021**, *35*, No. 106948.
(37) Yau, M. Q.; Liew, C. W. Y.; Toh, J. H.; Loo, J. S. E. A head-to-head comparison of MM/PBSA and MM/GBSA in predicting binding affinities for the CB(1) cannabinoid ligands. *J. Mol. Model* **2024**, *30*, 390.
(38) Unni, S.; et al. Web servers and services for electrostatics calculations with APBS and PDB2PQR. *J. Comput. Chem.* **2011**, *32*, 1488−1491.
(39) Jurrus, E.; et al. Improvements to the APBS biomolecular solvation software suite. *Protein Sci.* **2018**, *27*, 112−128.
(40) Kothiwale, S.; Borza, C. M.; Lowe, E. W., Jr.; Pozzi, A.; Meiler, J. Discoidin domain receptor 1 (DDR1) kinase as target for structure-based drug discovery. *Drug Discov Today* **2015**, *20*, 255−261.
(41) Canning, P.; et al. Structural mechanisms determining inhibition of the collagen receptor DDR1 by selective and multi-targeted type II kinase inhibitors. *J. Mol. Biol.* **2014**, *426*, 2457−2470.

https://doi.org/10.1021/acsmedchemlett.4c00634
ACS Med. Chem. Lett. 2025, 16, 602−610